Oral Microbiology Immunology 2008: 23: 70–78
Printed in Singapore. All rights reserved

ORAL MICROBIOLOGY
AND IMMUNOLOGY

Role of *gap3* in Fap1 glycosylation, stability, *in vitro* adhesion, and fimbrial and biofilm formation of *Streptococcus parasanguinis*

Z. Peng[1,2], H. Wu[1,4], T. Ruiz[3], Q. Chen[1], M. Zhou[1,4], B. Sun[1], P. Fives-Taylor[1]

[1]Department of Microbiology and Molecular Genetics, University of Vermont, Burlington, USA, [2]Center of Stomatology, Tongji Hospital, Tongji Medical College, Huazhong University of Science and Technology, Wuhan, China, [3]Departments of Molecular Physiology and Biophysics, University of Vermont, Burlington, VT, USA, [4]Departments of Pediatric Dentistry and Microbiology, Schools of Dentistry and Medicine, University of Alabama, Birmingham, AL, USA

Peng Z, Wu H, Ruiz T, Chen Q, Zhou M, Sun B, Fives-Taylor P. Role of gap3 *in Fap1 glycosylation, stability,* in vitro *adhesion, and fimbrial and biofilm formation of* Streptococcus parasanguinis.
Oral Microbiol Immunol 2008; 23: 70–78. © 2008 The Authors. Journal compilation © 2008 Blackwell Munksgaard.

Background/aims: *Streptococcus parasanguinis* is a primary colonizer of the tooth surface. Its adhesion is mediated by the long fimbriae, which are composed of multiple subunits of a serine-rich glycoprotein, Fap1. Previous studies revealed that a chromosomal region located downstream of *fap1* is involved in the secretion and glycosylation of Fap1. In this study, we investigated the role of a glycosylation-associated gene, *gap3*, in Fap1 biogenesis.
Methods: A *gap3* non-polar mutant was constructed by insertional inactivation. The phenotype of the mutant and the subcellular distribution of its products were investigated. The binding ability of the mutant was tested with saliva-coated hydroxyapatite (SHA). Electron microscopy was used to observe the morphological changes on the mutant cell surface. Confocal microscopy was utilized to determine biofilm formation ability.
Results: The *gap3* mutant produced a partially glycosylated Fap1 precursor, that was less stable than mature Fap1. The Fap1 precursor was distributed in all subcellular fractions including the cell surface and culture medium although in decreased amounts. These data suggest a role for Gap3 in Fap1 glycosylation as well as a link between glycosylation and secretion of Fap1. The *gap3* mutant had reduced binding to saliva-coated hydroxyapatite. Electron microscopy revealed that the *gap3* mutant had lost its long fimbriae. Biofilm formation was also inhibited by the *gap3* mutation. Fewer *gap3* mutant cells adhered to the biofilm surface and microcolony formation was decreased.
Conclusion: Gap3 is required for the complete glycosylation and secretion of Fap1, which is important for fimbrial assembly, bacterial adhesion, and *in vitro* biofilm formation.

Key words: Fap1; fimbriae; glycosylation; high-molecular-weight serine-rich proteins; *Streptococcus parasanguinis*

Hui Wu, Department of Pediatric Dentistry, School of Dentistry, University of Alabama at Birmingham, Birmingham, AL 35294, USA
Tel.: +1 205 996 2392;
fax: +1 205 975 6251;
e-mail: hwu@uab.edu
Accepted for publication May 27, 2007

The sanguis streptococci comprise a large proportion of the oral bacterial species found in dental plaque. They are early colonizers of the tooth surface (28, 35) and can act as a substratum to co-aggregate with other oral bacteria that are important for dental plaque formation (2, 5, 18). The adhesion of *Streptococcus parasanguinis* FW213 to an *in vitro* tooth surface model, saliva-coated hydroxyapatite (SHA), is mediated by long peritrichous fimbriae (11). Fap1, a 200 kDa streptococcal surface glycoprotein, is the major subunit of the long fimbriae, and is involved in bacterial adhesion to SHA (30, 38). Fap1 is a member of a new, high-molecular-weight serine-rich glycoprotein family that was recently discovered within

gram-positive bacteria such as streptococci and staphylococci. Some members of this family include PsrP in *Streptococcus pneumoniae* (34), SrpA in *Streptococcus cristatus* and *Streptococcus sanguis* (16, 24), Hsa and GspB in *Streptococcus gordonii* (1, 31), SraP in *Staphylococcus aureus* (27) and Srr-2 in *Streptococcus agalactiae* (19).

A large chromosomal region is dedicated to Fap1 biosynthesis. This pathogenicity island contains a seven-gene cluster located immediately downstream of *fap1* (39). This cluster includes *secY2*, *orf1*, *orf2*, *orf3*, *secA2*, *gtf1* and *gtf2*, which are differentially involved in Fap1 glycosylation and secretion. Gene clusters, such as this, have also been found in the aforementioned and in other gram-positive bacteria. They are involved in the transport of the large, serine-rich, cell wall-anchored proteins, such as Fap1. Some of the genes have been characterized as an accessory secretory system in *S. gordonii* (1, 33). The system differs significantly from the general secretory pathway, the cannonical Sec system, which is used by bacteria for the secretion of proteins (10).

Studies in our laboratory demonstrated that one of the accessory secretion components, SecA2, is required for Fap1 secretion (3, 4). The glycosyltransferases Gtf1 and Gtf2 are essential for Fap1 glycosylation and SecY2 is required for the complete glycosylation of Fap1 (39).

Little is known about the role of the other genes in the locus to Fap1 biogenesis. In this study, we chose to investigate the role of one open reading frame, *orf3*, in the *secY2/gtf2* locus. It was renamed *gap3* in this study because characterization of a non-polar *gap3* mutant indicated that Gap3 had a role in Fap1 glycosylation.

Materials and methods

Bacterial strains, media, and growth conditions

The bacterial strains, plasmids, and antibodies used are listed in Table 1. Frozen *S. parasanguinis* strains preserved with 5% dimethyl sulphoxide were streaked on to Todd–Hewitt (TH) agar (Difco Laboratories, Detroit, MI) plates, and incubated for 15–18 h in the presence of 5% CO_2 at 37°C. Liquid cultures were prepared by inoculating single colonies from TH agar plates into TH broth; these were then grown statically in 5% CO_2 at 37°C. Desired cell concentrations were determined from a growth curve with absorbance at 470 nm. *Escherichia coli* were cultured in Luria–Bertani (LB) medium (Difco Laboratories). Antibiotics were used at the following concentrations: 10 μg/ml erythromycin and 125 μg/ml kanamycin in TH broth or agar plates for *S. parasanguinis*; 500 μg/ml erythromycin and 25 μg/ml kanamycin in LB broth or agar plates for *E. coli*.

Table 1. Bacterial strains, plasmids and antibodies used in this study

Strain, plasmid or antibody	Relevant characteristics	Reference or source
Strains		
S. parasanguinis		
FW213	Wild type	(11)
VT1393	*fap1::aphA-3*, null mutant of *fap1*, Kan^R	(38)
VT1619	*gap3* insertion mutant, Kan^R	This study
VT1686	pVPT1686 into VT1619, *gap3* complementation strain, Erm^R	This study
VT1687	pVPT into VT1619, vector control strain, Erm^R	This study
E. coli		
DH10B	Host strain for cloning	Invitrogen
JM109	Host strain for cloning	Invitrogen
Plasmids		
pVPT	An *E. coli* and *S. parasanguinis* shuttle vector, parent of pVPT1686	This study
pVT1607	pGEM Teasy vector contained *gap3* gene	This study
pVT1610	*gap3* deletion plasmid from pVT1607	This study
pVT1613	*aphA-3* kanamycin cassette cloned into pVT1610	This study
pVT1616	Deletion of Amp^R cassette from pVT1613	This study
pVPT1686	For Gap3 complementation	This study
Antibodies		
D10	Partially glycosylated Fap1 glycan epitope-specific mAb	(6)
E42	Fap1 peptide epitope-specific mAb	(6)
F51	Mature Fap1 glycan epitope-specific mAb	(6)
Anti-SecA2 serum	SecA2-specific Ab	(4)
Anti-Tpx serum	Thiol peroxidase-specific Ab	(29)

General DNA techniques

S. parasanguinis FW213 genomic DNA was isolated using the Puregene DNA Isolation Kit (Gentra System, Minneapolis, MN). Standard recombinant DNA techniques were used for DNA preparation and analyses, as described by Sambrook et al. (26). Plasmid DNA preparations were isolated with QIAprep Miniprep Kit (Qiagen, Valencia, CA). Polymerase chain reaction (PCR) was carried out with Taq DNA polymerase (Invitrogen, San Diego, CA). PCR products were purified with a QIAquick PCR Purification Kit (Qiagen). Competent cells for *S. parasanguinis* electroporation were prepared as described previously (8).

Construction of the *gap3* mutant

A *gap3* mutant was constructed by allelic replacement of *gap3* with a kanamycin resistant cassette, *aphA-3* (aminoglycoside phosphotransferase). Briefly, a fragment containing the *gap3* gene and its flanking regions was amplified from *S. parasanguinis* chromosomal DNA using corresponding primers (5′-CTCAATTTCTCTAGGATAC-3′ and 5′-GAGCGGTACTTGTCGTATAC-3′). The PCR fragment was ligated into pGEM-T easy to generate pVT1607. A 400-base-pair region of *gap3* was deleted from pVT1607 by inverse PCR using a pair of *Hin*dIII embedded primers (Primer 1: 5′-GATC***AAGCTT***TGGTACAGCATCAATCTGATACTC-3′ and Primer 2: 5′-GTAG***AAGCTT***CCGAAGGATCTTGATTTGGTG-3′). The inverse PCR product was digested with *Hin*dIII and self-ligated to form pVT1610. A plasmid, pVT1613, was constructed by ligation of a promoterless *aphA-3* kanamycin-resistant cassette with *Hin*dIII-digested pVT1610. The plasmid pVT1616 was generated by deletion of the Amp^R cassette from pVT1613. Finally, the *gap3* insertional mutant VT1619 was constructed by transformation of FW213 with pVT1616, followed by selection of kanamycin-resistant colonies. Presence of the correct mutation in VT1619 was determined by PCR amplification of *gap3* from the *gap3* mutant chromosomal DNA using Gap3upF and Gap3downR primers (5′-CCGCCGTCGACATGACTAAACAGTTAATTTC-3′, 5′-CGC***GGATCC***TTAAATATATTCTATTAAA-3′). Another PCR using the same forward primer Gap3upF, and a different reverse primer specific for *aphA-3* (*aphA-3* R, 5′-GCTAACGCTCC-

TAAAACTTG-3′) was carried out to confirm the presence of *aphA-3* in the targeted region. The in-frame insertion was further examined by DNA sequencing analyses with amplified PCR products. A Western blot analysis probed with antiserum against SecA2, a protein encoded by a gene downstream of *gap3*, was performed to confirm that the mutation in VT1619 was non-polar.

Detection of expression of *gap3*-kanamycin allele in the *gap3* mutant by reverse transcription PCR

To examine the expression of the *gap3*-kanamycin cassette by the *gap3* mutant, total RNAs were isolated from *S. parasanguinis* FW213 and the *gap3* mutant using TRIzol reagent and following the manufacturer's instructions (Invitrogen). First, 20 μg RNA was treated with DNaseI (Amersham, Buckinghamshire, UK) to remove contaminating DNA. The treated RNA was then precipitated. For *in vitro* reverse transcription reactions, the DNaseI-treated RNA and 5 pmol specific *gap3* reverse primer *gap3*-KpnI-R (5′-GATCAGGTACCAATATATTCTATTAAATTTTTC-3′) were mixed and denatured at 70°C for 5 min, and then quickly chilled on ice. Subsequently, 1 × Moloney lurine leukemia virus (M-MLV) buffer (Promega, Madison, WI), 5 mM dNTP, 10 U RNasin (Promega) and 160 U M-MLV reverse transcriptase (Promega) were added to the above mixture to a total volume of 20 μl and incubated at 42°C for 1 h. The reaction was terminated by heating at 94°C for 5 min. Finally, the *in vitro* reverse-transcribed product was diluted and used for PCR amplification with *gap3*-specific forward and reverse primers (forward primer *gap3-Sal*I-F: 5′-GATCAGTCGACATGACTAAACAGTTAATTTC-3′; reverse primer *gap3-Kpn*I-R).

Complementation of the *gap3* mutant

An *E. coli*-streptococcal shuttle plasmid, pVPT containing *gap3* was used to complement the *gap3* mutant. A PCR product of *gap3* was amplified with *Sal*I and *Bam*HI embedded Gap3upF and Gap3downR primers as previously described, then digested with *Sal*I and *Bam*HI and ligated into linearized pVPT downstream of a functional streptococcal promoter to construct recombinant plasmid, pVT1686. The pVT1686 was transformed into VT1619, the *gap3* mutant, by electroporation. A negative control strain, VT1687 was constructed by transformation of the *gap3* mutant with empty vector pVPT. Western blot analysis was performed with a peptide-specific monoclonal antibody (mAb) E42, and two glycan-specific mAbs, D10 and F51 (6, 30), to determine if Fap1 biogenesis was restored in the complemented *S. parasanguinis* strains. A 443-kDa horse-spleen apoferritin (Sigma, A3660-1VL) was used on SDS gels, followed by staining with Ponceau S solution (Sigma, P7170) on transferred membrane to make an estimation of the position of the high-molecular-weight Fap1 precursor.

Subcellular fractionation

S. parasanguinis cells, in early log phase of exponential growth (A_{470} = 0.4), were harvested by centrifugation at 5000 ***g***, 4°C for 10 min. The cell culture supernatant was stored at 4°C for culture medium protein extraction. The cell pellet was resuspended in phosphate-buffered saline (PBS, 137 mM NaCl; 2.7 mM KCl; 11.9 mM phosphates, pH 7.3) with a protease inhibitor cocktail (PIC, Sigma-Aldrich). The cells were lysed either by two cycles using a French Press minicell (Thermo Spectronic, Waltham, MA) at 20,000 p.s.i. or by treatment with amidase at 10 μg/ml. The lysates were centrifuged at 20,000 ***g***, 4°C for 15 min to remove insoluble debris. The lysate was further centrifuged at 100,000 ***g***, 4°C for 2 h to separate the membrane fraction from the cytoplasm. To prevent membrane fractions from possible cross-contamination by cytoplasmic fractions, the pellet containing the membrane protein was washed with PBS, centrifuged at 13,000 ***g***, 4°C twice. The pellet was resuspended in PBS + 1%CHAPS [(3-cholamidopropyl) dimethylammonio-1-propane sulfonate]. The culture medium protein sample was extracted from the supernatant of cell culture by precipitation with two volumes of ice-cold ethanol. The mixture was incubated at −80°C for 10 min to precipitate the proteins. After centrifugation at 17,500 ***g***, 4°C for 10 min, the pellet was air-dried and dissolved in 50 mM carbonate buffer (16 mM sodium carbonate, 34 mM sodium bicarbonate, pH 9.75). The extraction of streptococcal cell wall-associated protein was performed as described previously (22). Briefly, the cells were harvested by centrifugation at 5000 ***g***, 4°C for 10 min. The pellet was resuspended in TEP buffer [10 mM Tris–HCl, 1 mM ethylenediaminetetraacetic acid, 1 mM phenylmethylsulfonyl fluoride (PMSF), pH7.5], centrifuged at 5000 ***g***, 4°C for 2 min. The supernatant was removed and the cells were washed by suspension and centrifugation alternately. Cells were spheroplasted by addition of spheroplasting buffer (2 mM Tris–HCl, pH 7.5, 1 mM $MgCl_2$ and 43.7 mM raffinose, 1 mM PMSF, pH6.8). The cells were resuspended by vortex-mixing and mutanolysin (Sigma-Aldrich) was added. The cells were incubated for 30 min at 37°C and then centrifuged at 5000 ***g***, 4°C for 10 min. The supernatant was transferred to a clean tube to isolate the cell wall-associated proteins. The protein concentrations of all fractions were determined by bicinchoninic acid (BCA) assays (Pierce, Rockfort, IL).

Protein stability experiment

S. parasanguinis cells were grown to A_{470} = 0.4; 100 μg/ml chloramphenicol was added to cultures. Samples were then taken at various time-points: 0, 20 min, 40 min, 1 h, 2 h, and 4 h. Each sample was centrifuged at 4°C to obtain the cell pellet, and was frozen in liquid nitrogen and stored at −80°C. Whole cell lysates were prepared from collected cell pellets as mentioned above. Western blot was performed with a peptide-specific mAb E42 that recognizes all forms of Fap1. The amount of protein used for loading for all samples was normalized to 20 μg per well.

Electron microscopy

S. parasanguinis cell cultures (5 ml) grown to A_{470} = 0.4, were harvested by centrifugation. Cell pellets were washed twice with 1 ml ice-cold PBS and resuspended in 100 μl PBS. A small sample (5 μl) of the bacterial suspension was diluted in PBS to a concentration that provided good coverage on the grid and was applied to 400 mesh copper grids coated with a thin carbon film. The grids were first washed by gently streaming several drops of PBS buffer over the grids. They were negatively stained by running a few drops of 2% phosphotungstic acid, pH 7 with NaOH (Ted Pella, Redding, CA) over the grid surfaces. The last drop was left on the grids for 30 s. Finally, the excess liquid was wicked off and the grids were fast air-dried.

The grids were observed on a Tecnai 12 Philips electron microscope (FEI, Eindhoven, the Netherlands) equipped with a LaB6 cathode operated in point mode (Kimball, Wilton, NH), and a 14-μm 2048 CCD camera (TVIPS, Gauting, Germany). The microscope was run under identical conditions as have been used in the past to obtain images that show Thon rings beyond

0.9 nm resolution in vitreous ice preparations (25). Images were recorded at an accelerating voltage of 100 kV and at nominal magnifications in the range 40,000 × to 70,000 × under low-dose conditions on either film (S0-163 Kodak) or the CCD camera. Images were converted to SPIDER format (12) and a high-pass filter was used to remove the long-range background variations caused by uneven staining.

Adhesion assay

An *in vitro* tooth model, SHA was used to test the effects of *gap3* mutagenesis on *S. parasanguinis* adhesion as described previously (7). Briefly, [^{3}H]thymidine-labeled bacteria (5×10^8) in adhesion buffer (67 mM phosphate buffer, pH 6.0) were sonicated for 15 s at 85 W using an ultrasonic cuphorn system (Heat systems-Ultrasonics, Farmingdale, NY). A 1-ml sample of sonicated bacteria (in triplicate) was added to 10-ml scintillation vials containing SHA and incubated for 1 h at 37°C with gentle shaking. The beads were allowed to settle and the supernatant fluids were removed. The beads were washed three times with adhesion buffer. The amounts of unbound bacteria in the supernatant fluids and of bacteria bound to SHA were determined in a Wallac 1400 liquid scintillation counter.

Biofilm assays

S. parasanguinis and the *gap*3 mutant were grown overnight in TH broth, diluted 1 : 100 in TH + 1% glucose culture medium and grown to mid-logarithmic phase; 15 ml of the culture was transferred to a 50-ml Corning centrifuge tube containing a vinyl coverslip (Structure Probe, Inc., West Chester, PA). Biofilm formation on the vinyl coverslip was assayed after 6 h at 37°C in 5% CO_2 without shaking. The vinyl coverslips were removed, rinsed with PBS and the remaining cells were stained with 1 ml of 10 μM green fluorescent nucleic acid stain SYTO 9 (Molecular Probes, Eugene, OR) for 15 min. The biofilm was rinsed twice with PBS to remove unbound stains and to reduce background fluorescence. The stained biofilms were imaged using laser scanning confocal microscopy (CLSM). The fluorescence was excited at the selected location with the 488-nm argon laser and the resulting signal was assigned the color green.

Results

Non-polar insertional mutagenesis of *gap3*

The role of *gap3* in Fap1 biogenesis was investigated. A *gap3* in-frame insertional mutant was constructed as described in the Materials and methods and illustrated in Fig. 1(A). A 0.71-kilobase (kb) fragment was amplified from the *gap3* mutant using one primer located upstream of *gap3* (Gap3upF) and the other one specific for the inserted kanamycin-resistant cassette *aphA-3* (aphA-3R) (Fig. 1B, lane 1). No PCR product was generated from the wild-type bacteria with the same pair of primers (Fig. 1B, lane 2), suggesting that the kanamycin cassette was inserted into the *gap3* region. PCR analysis with primers flanking the *gap3* gene (Gap3upF and Gap3downR) revealed a PCR fragment of

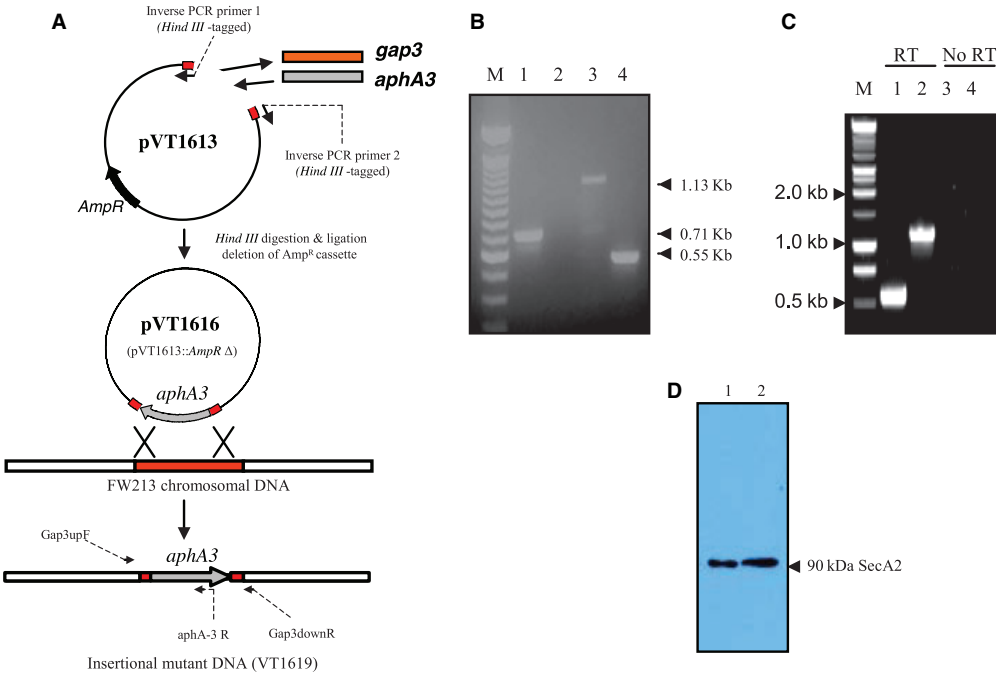

Fig. 1. Non-polar allelic replacement mutagenesis of *gap3* in *Streptococcus parasanguinis*. (A) Schematic diagram of construction of the *gap3* insertional mutant. The *gap3* gene with flanking regions was cloned into pGEM Teasy plasmid, the *gap3* open reading frame was deleted and replaced with a kanamycin-resistant cassette *aphA-3* to generate pVT1613. pVT1616 was generated by deletion of an ampicillin-resistant cassette from pVT1613. The *gap3* mutant VT1619 was constructed by transformation of pVT1616 into FW213 and selected by its kanamycin-resistance. (B) PCR analysis of the *gap3* insertional mutation. Chromosomal DNA from mutant VT1619 (lanes 1 and 3), and wild-type *S. parasanguinis* FW213 (lanes 2 and 4) were used as PCR templates. A pair of primers, the forward one (Gap3upF) corresponding to the *gap3* upstream region and the reverse one (*aphA-3* R) specific to *aphA-3*, was used to amplify a *gap3* and *aphA-3* junction fragment (lanes 1 and 2). Gap3upF and another reverse primer (Gap3downR) corresponding to the *gap3* downstream region were used to amplify a fragment flanking the *gap3* gene (lanes 3 and 4); M, 100-base-pair ladder. (C) RT-PCR analysis of the *gap3* mutant. Total RNA was isolated from FW213 (lanes 1 and 3) and VT1619 (lanes 2 and 4) and treated with DNAaseI to remove the contaminating DNA, the treated RNA samples were subjected to reverse transcription in the presence of reverse transcriptase (RT) (lanes 1 and 2) and absence of RT (lane 3 and 4) and then analysed by PCR for the transcription of wild-type and mutant *gap3* alleles. (D) Western blot analysis of SecA2 expression. The whole cell protein extracts from FW213 (lane 1) and VT1619 (lane 2) were probed with anti-SecA2 serum. Arrow indicates 90-kDa SecA2.

1.13 kb in the mutant (Fig. 1B, lane 3) and a smaller PCR fragment of 0.55 kb in the wild-type strain (Fig. 1B, lane 4). These results confirmed the insertion of the kanamycin-resistant cassette in the intended *gap3* region. The accuracy of the mutation was confirmed by DNA sequencing (data not shown). The expression of *aphA-3*-interrupted *gap3* in the *gap3* mutant was examined with RT-PCR. The wild-type FW213 expressed a 0.5-kb fragment consistent with the portion of Gap3 before the insertion of *aphA-3* (Fig. 1C, lane 1). The *gap3* mutant expressed the expected 1.2-kb fragment (Fig. 1C, lane 2).

The expression of a downstream gene, *secA2*, was assessed to determine if the mutation was non-polar. A Western blot showed that the mutant and wild-type bacteria expressed comparable levels of SecA2 (Fig. 1D, lanes 1 and 2), indicating that the *gap3* mutation was non-polar.

The *gap3* mutant failed to produce mature Fap1 but yielded a partially glycosylated Fap1 precursor

A Western blot probed with monoclonal antibody E42 (peptide-specific) showed that the wild-type FW213 produced the mature Fap1 protein, a 200-kDa band (Fig. 2A, lane 1). The *gap3* mutant did not produce the 200-kDa mature Fap1, instead it generated a new Fap1 species that migrated at approximately 470 kDa (Fig. 2A, lane 2). This high-molecular-weight species reacted with one glycan-specific mAb D10 (Fig. 2B, lane 2), but failed to react with the other glycan-specific mAb F51 (Fig. 2C, lane 2), which only recognizes the mature Fap1. We performed complementation experiments to verify that the observed Fap1 defects were attributed to the loss of *gap3*. Expression of mature Fap1 migrating at the position of 200 kDa was restored in the *gap3* complemented strain VT1686. This mature species was detected by all Fap1-specific mAbs (Fig. 2A–C, lane 3). No mature Fap1 was observed in the strain VT1687 carrying the empty vector pVPT (Fig. 2A–C, lane 4).

We previously showed that F51 and D10 mAbs reacted with different glycan epitopes on Fap1, while E42 mAb reacted with peptide epitopes on Fap1 (6, 30, 39). F51 recognizes the mature 200-kDa protein while D10 recognizes a partially glycosylated species as well as the mature one. Taken together, these results indicate that the 470-kDa protein generated by the *gap3* mutant is only partially glycosylated and Gap3 plays either a direct or an indirect role in Fap1 glycosylation.

Subcellular localization of mature Fap1 and partially glycosylated Fap1 precursor

Fap1 subcellular distribution was characterized in both the *gap3* mutant VT1619 and the wild-type strain FW213. Four subcellular fractions, cytoplasmic, membrane, cell-wall associated, and culture medium (supernatant), were prepared. Proteins from each fraction were analysed by Western blot with Fap1-specific mAbs E42, F51 and D10. The Fap1 protein profile from each fraction was shown in Fig. 3. All four fractions prepared from FW213 expressed mature Fap1. The result was consistent with previous work suggesting that Fap1 glycosylation happens before its secretion (3). Interestingly, the 470 kDa Fap1 precursor produced by the *gap3* mutant was also found in all fractions, including the supernatant, albeit the production level was reduced. These data indicate that Gap3 has an important role in the complete glycosylation of Fap1. Fap1 is glycosylated in the cytoplasm (3) and as this partially glycosylated intermediate is exported at a reduced level, it also suggests that complete glycosylation and secretion of Fap1 may be linked.

To ensure that the other subcellular fractions were not contaminated by cytoplasmic protein samples, the presence of thiol peroxidase (Tpx), a cytoplasmic-specific protein, was used as a control to assess the purity of the subcellular fractions. This 20-kDa Tpx protein lacks a signal peptide and previous data showed that it exists exclusively in cytoplasmic regions (9, 29). A polyclonal antibody against Tpx was used to probe the subcellular fractions in both FW213 and VT1619. No Tpx was detected in the membrane, cell-wall-associated proteins, and supernatant fractions by Western blots, while it was readily detected in the cytoplasmic fractions of both FW213 and VT1619 with a similar signal intensity (Fig. 3D).

The partially glycosylated Fap1 was less stable than mature Fap1

Glycosylation of some proteins protects them from degradation (14, 36). A time–course experiment using chloramphenicol to inhibit new bacterial protein synthesis (15, 21, 23) was used to investigate the stability of the 200-kDa and the 470-kDa forms of Fap1, E42 was used to detect the immunoblot signal strength of protein bands at different time-points. The Western blot data clearly showed that the intensity of the 200-kDa mature Fap1 did not decrease during the time–course after inhibition of protein synthesis, while the 470-kDa form was diminished after 1 h (Fig. 4). The smear below the 470-kDa Fap1 bands also suggested that an active degradation process was happening. As glycosylation stabilizes proteins and protects them from degradation (14, 36), these data are also consistent with incomplete glycosylation in the 470-kDa form.

The *gap3* mutant lost the typical long fimbriae

Fap1 is essential for fimbrial biogenesis (38). The above data demonstrated that

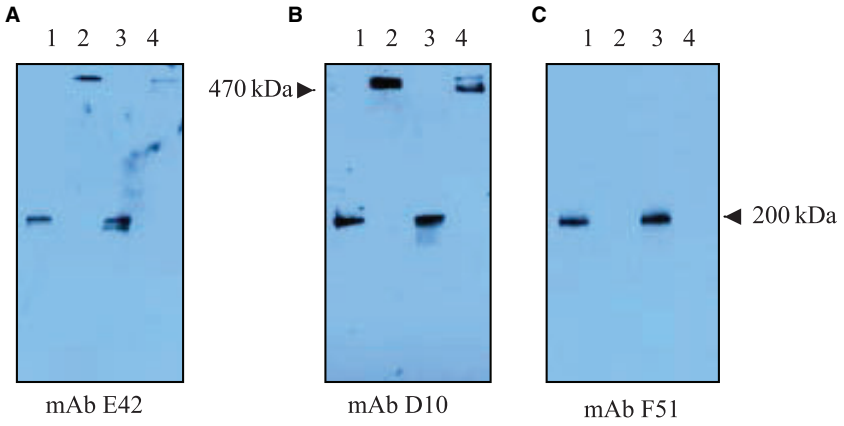

Fig. 2. Western blot analysis of Fap1 expression. Whole cell extracts of the same amounts of proteins prepared from wild-type strain FW213 (lane 1), *gap3* mutant VT1619 (lane 2), *gap3* complemented strain VT1686 (lane 3), and vector control strain VT1687 (lane 4) were probed with three Fap1-specific mAbs F51, E42, and D10.

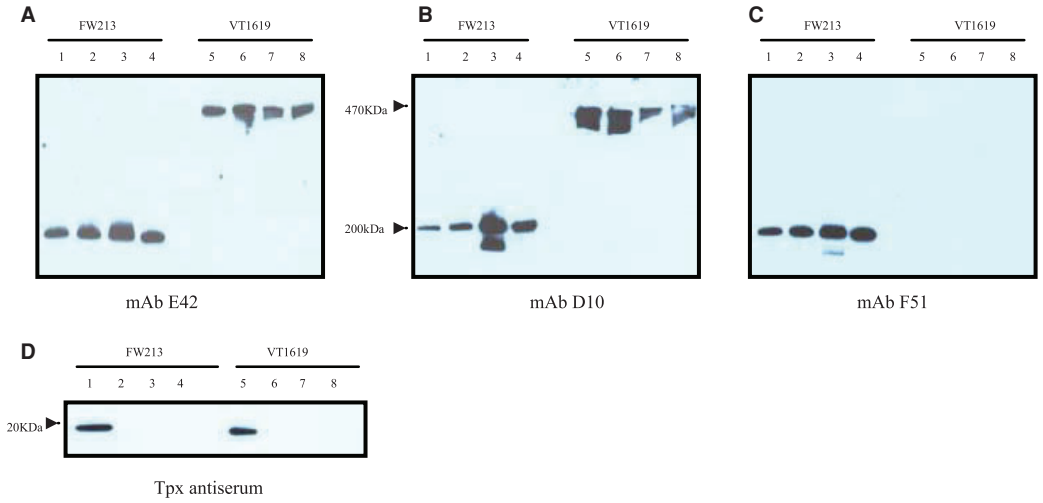

Fig. 3. Subcellular localization of Fap1. Cell fractions including the cytoplasmic (lanes 1 and 5), membrane (lanes 2 and 6), and cell wall-associated protein (lanes 3 and 7) and the supernatant fractions (lanes 4 and 8) were prepared from wild-type FW213 (lanes 1–4) and the *gap3* mutant VT1619 (lanes 5–8), and subjected to Western blot analyses using mAbs E42 (A), D10 (B), F51 (C) and polyclonal anti-Tpx antibody (D).

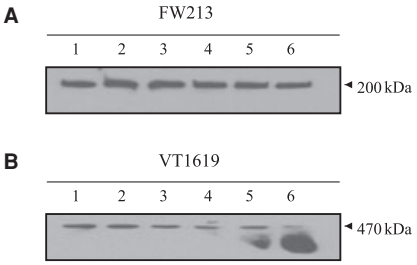

Fig. 4. Stability comparison between mature Fap1 and partially glycosylated Fap1 precursor. Lanes 1 to 6 are FW213 and VT1619 whole cell lysate from time-points 0, 20 min, 40 min, 1 h, 2 h, and 4 h after adding 100 μg/ml chloramphenicol. Sample loading amount was 20 μg per well. Western blot was performed with mAb E42.

Gap3 played a role in Fap1 glycosylation. We examined the bacterial surface morphology of the *gap3* mutant by transmission electron microscopy to investigate the function of Fap1 glycosylation in fimbrial formation. FW213 expressed the long fimbriae characteristic of the wild-type strain (Fig. 5A) (7, 38). Fimbriae were very flexible structures that bent easily in all the preparations. A close look at individual fimbriae revealed an internal substructure with a periodicity, which can be interpreted as arising from the single Fap1 subunits. In some cases several fimbriae were close together, forming a well-aligned raft that made the internal substructure more outstanding (Fig. 5A). The *gap3* mutant failed to express the long fimbriae, suggesting that the 470-kDa Fap1 species could not be assembled into long fimbriae (Fig. 5B). Short fimbriae, another type of fimbriae, were readily detected in this mutant because of the loss of the long fimbriae. These short fimbriae are similar to those detected on the *fap1* null mutant (VT1393) (Fig. 5C). When the *gap3* mutant was complemented with the wild-type gene it regained the typical long fimbriae (Fig. 5D). These data are consistent with our previous studies that revealed that mature Fap1 is essential for the formation of these long fimbriae (13, 30, 38).

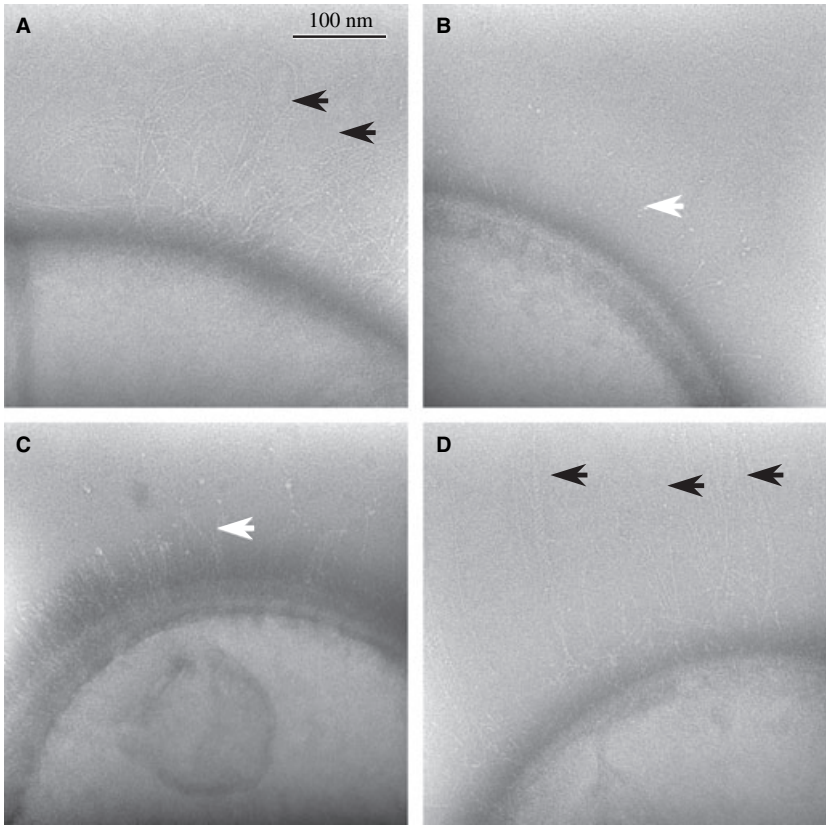

Fig. 5. Electron micrographs of whole-mount *Streptococcus parasanguinis* bacteria. *S. parasanguinis* bacteria, FW213 (A), VT1619 (B), VT1393 (C), and VT1686 (D), were placed on grids, negatively stained with 2% phosphotungstic acid pH 7.0 and visualized by electron microscopy. Black arrows point to the long fimbriae. White arrows point to the short fimbriae. Scale bar = 100 nm.

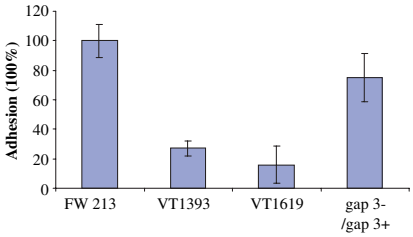

Fig. 6. Adhesion of FW213 and its mutants to SHA: bacteria were labeled with [^{3}H]thymidine and grown to OD_{470} = 0.6. Cells were resuspended, then added to 40 mg SHA and incubated at 37°C for 1 h. The beads and absorbed cells were allowed to settle, and the supernatant was removed. The amounts of radioactivity associated with beads and supernatant were determined in a Wallac 1400 liquid scintillation counter. The counts were converted to a percentage, with FW213 (wild-type strain) to be standard 100%. The data were obtained from three independent experiments in three replicates and are presented as means ± standard deviation. VT1393 is the *fap1* mutant; VT1619 is the *gap3* mutant; and *gap3*$^-$/*gap3*$^+$ is complemented mutant strain.

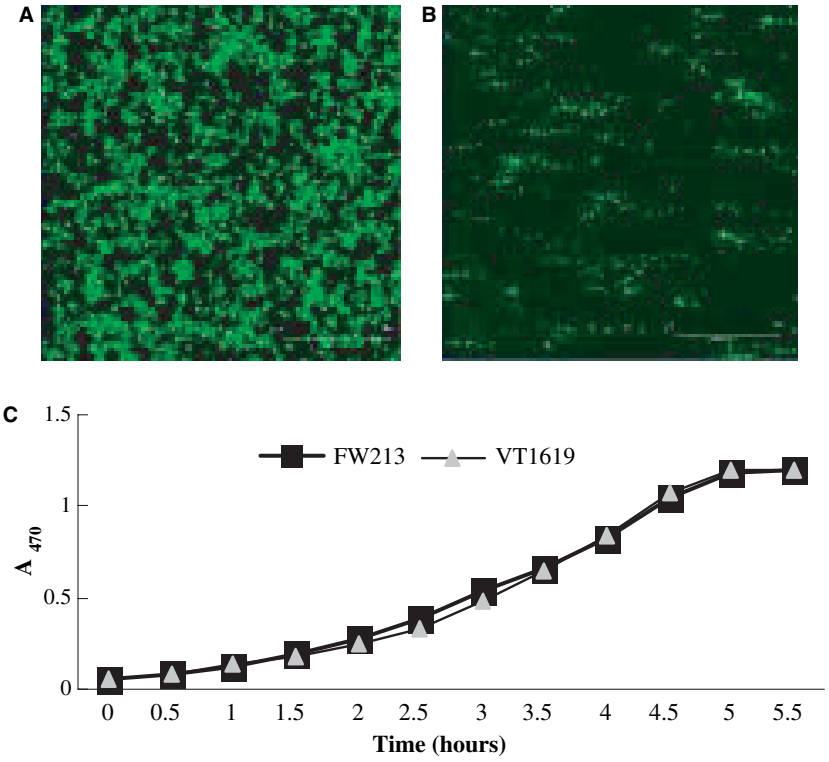

Fig. 7. Biofilm formation of *Streptococcus parasanguinis* analysed by Laser scanning confocal fluorescence microscopy. *S. parasanguinis* FW213 (A) and *gap3* mutant VT1619 (B) were allowed to grow on vinyl coverslips for 6 h to form biofilms. The coverslips were then washed, stained with green fluorescent nucleic acid stain. The stained biofilms were imaged using laser scanning confocal microscopy with the 488-nm argon laser. Bar = 50 μm The growth curve for the planktonic bacteria, FW213 and VT1619, was determined as described in Materials and methods and is depicted (C).

The *in vitro* adhesion ability of *gap3* mutant was decreased

In vitro binding experiments showed that the *gap3* mutant (VT1619) had >80% reduction in adhesion ability when compared to the wild-type strain FW213, while the *fap1* null mutant VT1393 had >70% reduction (Fig. 6), which was consistent with the previously published result (38). The *gap3*-complemented strain VT1686 had >75% recovery of adhesion function. This result showed the defective glycosylation of Fap1 caused by the *gap3* mutation affected *S. parasanguinis in vitro* adhesion activity.

The *gap3* mutation diminished *S. parasanguinis* biofilm formation

It has been demonstrated that flagella, pili, and fimbriae play important roles in the biofilm formation processes of many pathogenic microorganisms (20). These findings suggested that the main function of adhesins, pili, fimbriae, and flagella, is to initiate attachment and trigger the biofilm formation (17). We have shown that insertional inactivation of *fap1* caused a severe defect in biofilm formation of *S. parasanguinis* (13). The *gap3* mutant strain was assayed for its ability to form biofilms by laser scanning confocal fluorescence microscopy to determine if Gap3 played some role in bacterial biofilm formation. Numerous wild-type FW213 cells were found attached to the coverslip and formed many microcolonies (Fig. 7A). Fewer *gap3* mutant cells attached to the coverslip (Fig. 7B). The clusters formed by the mutant were smaller than those formed by the wild-type cells, suggesting that mature Fap1 is required for biofilm formation. Notably, no difference was observed in growth rates between wild-type and *gap3* mutant strains when the bacteria were grown under planktonic conditions (Fig. 7C). These results reinforce the concept that the Fap1-dependent long fimbriae are important for biofilm formation.

Discussion

Fap1 glycosylation and secretion are dependent on the expression of the *fap1* flanking gene cluster (39). The functions of SecA2, SecY2, Gtf1, and Gtf2 in Fap1 biogenesis have been investigated (3, 4, 39). However, the involvement of the other open reading frames in the processes has not been studied. In the present study, we sought to investigate the function of a gene downstream from *fap1*, *gap3*, in Fap1 biogenesis. A non-polar *gap3* mutant was constructed by in-frame insertional inactivation. Two glycan specific mAbs, F51 and D10 (6, 30), were utilized to determine changes in Fap1 glycosylation by the *gap3* mutation. The *gap3* mutant expressed a 470-kDa form of Fap1 that is positive for mAb D10, but does not bind to mAb F51, the mature Fap1-positive marker. These data suggest that the 470-kDa form of Fap1 is only partially glycosylated and that Gap3 plays a role in the glycosylation process. This Fap1 precursor was detected in all cellular fractions as well as at a reduced level in the culture medium. These data suggest that the loss of Gap3 does not inhibit secretion. As glycosylation of Fap1 takes place in the cytoplasm (3) it is more likely that the efficient secretion of Fap1 depends on its glycosylation. These results support the notion that Gap3 is critical for complete glycosylation of Fap1. Therefore we renamed the protein from Orf3 to Gap3 (glycosylation-associated protein 3).

The stability test result showed that the 470-kDa form of Fap1 was less stable than the 200-kDa mature form, suggesting that the defect in Fap1 glycosylation decreased Fap1 stability. It is known that glycosylation protects some proteins from degradation, and proteins with glycosylation defects tend to form inter-molecular cross-links, which affect their structural stability

(14, 36). Further investigation is required to clearly understand the role of Gap3 in Fap1 glycosylation and stabilization, and to determine if the effect is direct or indirect.

Fap1 is essential for fimbrial biogenesis (38). The *gap3* mutant failed to produce the long fimbriae that are typical on the cell surface of the wild-type strain (6, 7, 38) even though the 470-kDa Fap1 was exported (Fig. 5A,B). These data suggest that the assembly of fimbriae requires the fully glycosylated mature Fap1. To our knowledge this is the first time the degree of glycosylation has been noted to play a role in fimbrial biogenesis.

The adhesion of *S. parasanguinis* FW213 to SHA is mediated by long fimbriae (37, 38). Our study with SHA showed that the *gap3* mutation resulted in a diminution of bacterial adhesion. The reduction of binding activities between *gap3* and *fap1* mutants was similar, which suggests that the partially glycosylated Fap1 precursor produced by the *gap3* mutant contributed little to bacterial adhesion function. It is likely that the mutant's inability to assemble the long fimbriae plays the key role in this reduction of adhesion.

Biofilm formation of *S. parasanguinis* is also mediated by fimbriae (13). The genetic mutant of *gap3* formed biofilms with reduced biomasses, suggesting a role for Gap3 in biofilm formation. Adhesion to a substrate is the first step in biofilm formation. As we demonstrated a reduced adhesive ability for this mutant, it is not surprising that it did not adhere well to the coverslip, which is likely to be because of the loss of the long fimbriae. However, the inability to form larger microcolonies was also noted, even through the mutant grows at the same rate as the wild-type. At this stage of our investigations, it is not clear what steps have been affected to lead to this result. It is possible that the degree of glycosylation may play some role because it is known that polysaccharides play a role in the subsequent steps of biofilm formation (17). Further investigation is needed to determine the underlying mechanism. The short fimbriae were more obvious on the cell surface of both the *fap1* and *gap3* mutants because of the loss of the Fap1-related long fimbriae (Fig. 5B,C). These short fimbriae do not appear to play a role in the ability of the bacteria to adhere to the substrate; however, it is not known if they play a role in the reduced microcolony formation of the *gap3* mutant (Fig. 7). Currently, almost nothing is known about these short fimbriae on the *S. parasanguinis* cell surface. A genetic approach using transposon mutagenesis to characterize their function and biogenesis would be an interesting project.

A homologous *secY2/gtf2* locus is also required for the functional expression of the serine-rich glycoprotein, GspB of *S. gordonii* (1). *S. gordonii* possesses a Gap3 homologue, which bears 34% identity with *S. parasanguinis* Gap3. It was suggested that this protein was an accessory secretory protein and it was named Asp3 because the *asp3* mutant fails to secrete the GspB protein on the cell surface and in the culture supernatants. The 2004 report by Takamatsu et al. stated that GspB in the *asp3* mutant migrates to the same molecular mass position as the mature GspB and is accumulated intracellularly (32). This contradicts our results with Gap3. Our *gap3* mutant does not produce any mature Fap1 but rather expresses a high-molecular-weight 470-kDa species of Fap1. A more recent report by the same group suggests that they have now identified a high-molecular-weight GspB precursor in the mutants of some accessory secretory protein-encoding genes that is different from the mature form of GspB (33). This GspB precursor was found in the cell wall fraction, which is similar to our results with the Gap3 mutant. The glycosylation nature of this high-molecular-weight form of GspB is not known. It is possible that the GspB precursor is similar to the Fap1 precursor and is also partially glycosylated. Notably, we found that the concentration of the partially glycosylated Fap1 exported by the *gap3* mutant was significantly lower than that of the mature Fap1 on the FW213 cell surface and in the culture supernatant, suggesting that the secretion of the partially glycosylated Fap1 by the accessory secretion system is indeed not as efficient as the secretion of mature Fap1. Therefore, our findings are not mutually exclusive with the finding described for the function of Asp3. We determined that *gap3* plays an important role in Fap1 glycosylation. The results further indicate a role of glycosylation in Fap1 secretion. No findings about the effect of Asp3, the homologue of Gap3, on *S. gordonii* bacterial adhesion, fimbrial biogenesis, or biofilm formation has been reported.

In summary, we determined Gap3 functions in Fap1 biogenesis. We showed that Gap3 modulated Fap1 glycosylation, and that the glycosylation defect in the *gap3* mutant could inhibit the efficiency of secretion for the partially glycosylated Fap1 precursor. In addition, the mutation reduced *in vitro* bacterial adhesion, eliminated the assembly of long fimbriae on the cell surface, and diminished the biofilm formation of *S. parasanguinis*.

Acknowledgments

This work was supported by grants NIH/NIDCR R01-DE11000 and K22-DE14726 from the National Institute of Dental and Craniofacial Research. We thank Dr Keith Mintz for helpful comments and review of the manuscript, and Mr Ron Kimball and Tom Kellogg for help with the scintillation counter.

References

1. Bensing BA, Sullam PM. An accessory *sec* locus of *Streptococcus gordonii* is required for export of the surface protein GspB and for normal levels of binding to human platelets. Mol Microbiol 2002: **44**: 1081–1094.
2. Carlsson J, Grahnen H, Jonsson G et al. Establishment of *Streptococcus sanguis* in the mouths of infants. Arch Oral Biol 1970: **15**: 1143–1148.
3. Chen Q, Wu H, Fives-Taylor PM. Investigating the role of *secA2* in secretion and glycosylation of a fimbrial adhesin in *Streptococcus parasanguis* FW213. Mol Microbiol 2004: **53**: 843–856.
4. Chen Q, Wu H, Reetu K, Peng Z, Fives-Taylor PM. SecA2 is distinct from SecA in immunogenic specificity, subcellular distribution and requirement for membrane anchoring in *Streptococcus parasanguis*. FEMS Microbiol Lett 2006: **264**: 174–181.
5. Cisar JO, Brennan MJ, Sandberg AL. Lectin-specific interaction of *Actinomyces fimbriae* with oral streptococci. Washington, DC: American Society for Microbiology Press, 1985.
6. Elder BL, Fives-Taylor P. Characterization of monoclonal antibodies specific for adhesion: isolation of an adhesin of *Streptococcus sanguis* FW213. Infect Immun 1986: **28**: 421–427.
7. Fachon-Kalweit S, Elder BL, Fives-Taylor P. Antibodies that bind to fimbriae block adhesion of *Streptococcus sanguis* to saliva-coated hydroxyapatite. Infect Immun 1985: **28**: 617–624.
8. Fenno JC, Shaikh A, Fives-Taylor P. Characterization of allelic replacement in *Streptococcus parasanguis*: transformation and homologous recombination in a 'nontransformable' streptococcus. Gene 1993: **130**: 81–90.
9. Fenno JC, Shaikh A, Spatafora G et al. The *fimA* locus of *Streptococcus parasanguis* encodes an ATP-binding membrane transport system. Mol Microbiol 1995: **28**: 849–863.
10. Fernandez LA, Berenguer J. Secretion and assembly of regular surface structures in Gram-negative bacteria. FEMS Microbiol 2000: **24**: 21–44.
11. Fives-Taylor P. Isolation and characterization of a *Streptococcus sanguis* FW213

mutant nonadherent of saliva coated hydroxyapatite beads. In: Schlessinger D, ed. Microbiology–1982. Washington, DC: American Society for Microbiology, 1982: 206–209.
12. Frank J, Radermacher M, Penczek P, Zhu J, Li Y, Ladjadj M, Leith A. SPIDER and WEB: processing and visualization of images in 3D electron microscopy and related fields. J Struct Biol 1996: **116**: 190–199.
13. Froeliger EH, Fives-Taylor P. *Streptococcus parasanguis* Fimbria-associated adhesin Fap1 is required for biofilm formation. Infect Immun 2001: **69**: 2512–2519.
14. Gao Y, Mehta K. N-linked glycosylation of CD38 is required for its structure stabilization but not for membrane localization. Mol Cell Biochem 2007: **295**: 1–7.
15. Goodman SD, Gao Q. Firefly luciferase as a reporter to study gene expression in *Streptococcus mutans*. Plasmid 1999: **42**: 154–157.
16. Handley PS, Correia FF, Russell K et al. Association of a novel high molecular weight, serine-rich protein (SrpA) with fibril-mediated adhesion of the oral biofilm bacterium *Streptococcus cristatus*. Oral Microbiol Immunol 2005: **20**: 131–140.
17. Jefferson KK. What drives bacteria to produce a biofilm? FEMS Microbiol Lett 2004: **236**: 163–173.
18. Jenkinson HF, Lamont RJ. Streptococcal adhesion and colonization. Crit Rev Oral Biol Med 1997: **8**: 175–200.
19. Kyle NS, Elisabeth EA, April A et al. A unique serine-rich repeat protein (Srr-2) and novel surface antigen (ϵ) associated with a virulent lineage of serotype III *Streptococcus agalactiae*. Microbiology 2006: **152**: 1029–1040.
20. Lejeune P. Contamination of abiotic surfaces: what a colonizing bacterium sees and how to blur it. Trends Microbiol 2003: **11**: 179–184.
21. Lessard JL, Pestka S. Studies on the formation of transfer ribonucleic acid–ribosome complexes. XXIII. Chloramphenicol, aminoacyl-oligonucleotides, and *Escherichia coli* ribosomes. J Biol Chem 1972: **247**: 6909–6912.
22. McNab R, Jenkinson HF. Lipoproteins and other cell-surface associated proteins in streptococci. Methods Cell Sci 1998: **20**: 209–216.
23. Pestka S. Chloramphenicol. In: Corcoran JW, Hahn FE, ed. Antibiotics, **Vol. 3**. New York, NY: Springer-Verlag, 1975: 396–398.
24. Plummer C, Wu H, Kerrigan SW et al. A serine-rich glycoprotein of *Streptococcus sanguis* mediates adhesion to platelets via GPIb. Br J Haematol 2005: **129**: 101–109.
25. Ruiz T, Mechin I, Bar J, Rypniewski W, Kopperschlager G, Radermacher M. The 10.8-A structure of *Saccharomyces cerevisiae* phosphofructokinase determined by cryoelectron microscopy: localization of the putative fructose 6-phosphate binding sites. J Struct Biol 2003: **143**: 124–134.
26. Sambrook J, Fritsch EF, Maniatis T. Molecular cloning: a laboratory manual. Cold Spring Harbor, NY: Cold Spring Harbor Laboratory Press, 1989.
27. Siboo IR, Chambers HF, Sullam PM. Role of SraP, a serine-rich surface protein of *Staphylococcus aureus*, in binding to human platelets. Infect Immun 2005: **73**: 2273–2280.
28. Socransky SS, Manganiello AD, Propas D et al. Bacteriological studies of developing supragingival dental plaque. J Periodontal Res 1977: **12**: 90–106.
29. Spatafora G, Van Hoeven N, Wagner K, Fives-Taylor P. Evidence that GAP3 at the *Streptococcus parasanguis fimA* locus encodes a thiol-specific antioxidant. Microbiology 2002: **148**: 755–762.
30. Stephenson AE, Wu H, Novak J et al. The Fap1 fimbrial adhesin is a glycoprotein: antibodies specific for the glycan moiety block the adhesion of *Streptococcus parasanguis* in an in vitro tooth model. Mol Microbiol 2002: **43**: 147–157.
31. Takahashi Y, Konishi K, Cisar JO, Yoshikawa M. Identification and characterization of *hsa*, the gene encoding the sialic acid-binding adhesin of *Streptococcus gordonii* DL1. Infect Immun 2002: **70**: 1209–1218.
32. Takamatsu D, Bensing BA, Sullam PM. Genes in the accessory *sec* locus of *Streptococcus gordonii* have three functionally distinct effects on the expression of the platelet-binding protein GspB. Mol Microbiol 2004: **52**: 189–203.
33. Takamatsu D, Bensing BA, Sullam PM. Two additional components of the accessory Sec system mediating export of the *Streptococcus gordonii* platelet-binding protein GspB. J Bacteriol 2005: **187**: 3878–3883.
34. Tettelin H, Nelson KE, Paulsen IT et al. Complete genome sequence of a virulent isolate of *Streptococcus pneumoniae*. Science 2001: **293**: 498–506.
35. Tinanoff N, Gross A, Brand JM. Development of plaque on enamel. Parallel investigations. J Periodontal Res 1976: **11**: 197–209.
36. Upreti RK, Kumar M, Shankar V. Bacterial glycoproteins: functions, biosynthesis and applications. Proteomics 2003: **3**: 363–379.
37. Wu H, Fives-Taylor P. Identification of dipeptide repeats and a cell wall sorting signal in the fimbriae-associated adhesin, Fap1, of *Streptococcus parasanguis*. Mol Microbiol 1999: **34**: 1070–1081.
38. Wu H, Mintz KP, Ladha M, Fives-Taylor P. Isolation and characterization of Fap1, a fimbriae-associated adhesin of *Streptococcus parasanguis* FW213. Mol Microbiol 1998: **28**: 487–500.
39. Wu H, Su B, Peter N, Chen Q, Fives-Taylor P. Two gene determinants are differentially involved in the biogenesis of Fap1 precursors of *Streptococcus parasanguis*. J Bacteriol 2007: **189**: 1390–1398.